

Long-Lived Waveguides and Sound Wave Generation by Laser Filamentation

Liad Levi,^{*} Oren Lahav,^{*} Ido Kaminer, Mordechai Segev and Oren Cohen

Solid state institute and physics department, Technion, Haifa, Israel 32000

We discover long-lived (microsecond-scale) optical waveguiding in the wake of atmospheric laser filaments. We also observe the formation and then outward propagation of the sound wave. These effects may be used for remote induction of atmospheric long-lived optical structures from a far.

Propagation of self-guided laser filaments through air and other gases results in a rich variety of phenomena and applications [1-3]. A laser filament is formed when a femtosecond pulse with peak intensity above the critical power for collapse (3 GW in air at an optical wavelength of 800 nm) is propagating in a transparent medium [1]. In air, the diameter of a filament is approximately 100 μm and it can propagate over distances much longer than the Rayleigh length, from 10 cm up to the kilo-meter range [4-7]. A filament is formed due to a dynamic balance between the linear diffractive and dispersive properties of the medium and its nonlinear features such as the self-focusing optical Kerr effect and defocusing due to the free electrons released from the molecules through multi-photon ionization. In the atmosphere, filaments can be initiated at predefined remote distances [4,5] and propagate through fog, clouds and turbulence [8,9]. Thus, filaments are attractive for atmospheric applications such as remote spectroscopy [8,10] and laser-induced water condensation [11].

An atmospheric filament pulse initiates complex nonlinear dynamics in the densities of free electrons and ions, air density, and in the level of molecular alignment. However, all of these effects are generally believed to die out after ~ 10 nanoseconds. Experimental data about the long term dynamics is especially scarce. The filamenting pulse leaves behind free electrons at initial densities of 10^{16} - 10^{17} cm^{-3} [2,3], mostly from multi-photon ionization of oxygen molecules because the ionization potential of N_2 molecules is significantly larger (12 eV and 16 eV for O_2 and N_2 , respectively). Initially, the free electron density exhibits a radial bell-shape profile. It is now established that 100 picoseconds to ~ 1 nanosecond later, a shock wave of electron density is formed and is

propagating outward supersonically [12-15]. The resultant radially increasing plasma density can be used for guiding a delayed laser pulse [12-15] or a microwave pulse [16]. However, recombination between the free electrons and positive oxygen molecules decreases the plasma density by two orders of magnitude and limits this waveguiding effects to a few nanoseconds. Such nanosecond dynamics of charge carriers also results in the emission of a high power burst of terahertz radiation [17]. Subsequently, when the density of free electrons decreases to below 10^{14} cm^{-3} , the capture of free electrons by neutral oxygen molecules, with characteristic time of 150 nanoseconds, becomes the dominant process [5]. However, such negative oxygen ions are metastable. Indeed, it was demonstrated that a high energy nanosecond pulse can revive the plasma channel by detaching electrons from the negative oxygen ions - even several milliseconds after the passing of the initial femtosecond filamenting pulse [18]. The filamenting pulse also induces impulsive rotational excitation in the N_2 and O_2 molecules [19]. In particular, the molecules exhibit periodic revivals of molecular alignment for several tens of picoseconds after the passing of the filament pulse. Consequently, the refractive index of air undergoes anisotropic temporal modulation [20]. This mechanism was used for guiding properly delayed picosecond pulses [21,22].

Processes resulting from plasma or molecular alignment in the wake of atmospheric laser filaments are limited to the first few nanoseconds period. Consequently, it was generally believed that tens of nanoseconds after the filament, the medium does not exhibit any optical effect. Recently, however, it was discovered that 0.1-1 milliseconds after the filament, there is a circular negative index change that defocuses a probe beam [23]. This

effect was attributed to reduction in the air density at the center of the filament as a result of heating. The temporal resolution (~ 40 microseconds) in that experiment was set by an electronic shutter that controlled the input light to the CCD. As such, that experiment was insensitive to dynamics during the first several microseconds after the passing of the filamenting pulse.

Here, we use an electronically-delayed short optical pulse for probing the long-term effects generated by a femtosecond filamenting pulse in the atmosphere. We find that the filament induces a transient positive index-change lasting for approximately 1.5 microsecond. We demonstrate waveguiding through this induced positive index-change. In addition, we observe and study the formation of ultra-short acoustic waves and subsequently their outward propagation at the speed of sound.

The experimental setup is shown in Fig. 1. A "pump" Ti:Sapphire pulsed laser beam 1 cm wide with 50 fs time-duration, 1 mJ energy/pulse and at 1 KHz repetition rate is focused to a diameter of ~ 100 μm using a $f=100$ cm lens. The expected Rayleigh range of such a beam is of the order of 2 cm. Our beam forms a filament of ~ 30 cm length in the free air. We probe the filament wake using a weak pulsed laser beam of wavelength 527 nm, with 150 ns pulse-duration and 1 KHz repetition rate, which is triggered by the femtosecond laser. The delay between the probe and pump pulses is controlled electronically and can span a range of one msec. The pump and probe beams propagate in opposite directions. This setting helps in unraveling the induced index change, as the phase change accumulates along the filament, and at the same time the counter-propagation geometry

makes it easy to separate the probe beam from the pump beam. We define the "input" and "output" planes as the entrance and exit planes of the *probe* pulse, which is propagating within the channel induced by the filament. A lens, a movable 4f system and a CCD camera are used to image the probe beam at the input and output planes.

In the first experiment, we expand the probe beam such that it is approximately a plane wave at the input. Figures 2(a-f) show the intensity of the output probe beam for several delay times with respect to the filament pulse (where $\Delta t=0$ corresponds to time delay at which the centers of the probe and pump pulses collide in the filament region). The ratio between the peak intensity at the center (I_0) and the intensity in the uniform region (I_{BG}), as a function of the time delay, is shown in Fig. 2g. During the first 2/3 microseconds, the intensity of the output probe beam in the region of the center of the filament wake increases. The period within which the center is larger than the background lasts for approximately 1.55 microseconds. This intensity profile suggests the presence of a positive index change at the center of the filament wake, which "pulls" the light into the center. To test the positive index assumption, we check if the filament wake can guide our probe pulse. In this experiment, we insert a $f=100$ cm lens that focuses the probe beam into a diameter of ~ 100 μm at the input plane (Fig. 3a). When the pump beam is blocked, hence no filament is formed, the probe beam is propagating in free air and is broadening considerably due to diffraction (Fig. 3b). Figure 3c shows the intensity of the probe beam 0.8 μs after the pump pulse has created the 30 cm filament, clearly showing that the beam is indeed guided within the waveguide induced by the filament. Finally, Fig. 3d shows the fraction of power localized within the guiding region (a circle with

diameter of 300 microns) as a function of the time delay. This experiment unequivocally shows that the filament induces a positive index structure surviving ~ 1.5 microseconds after the 50 fsec filament pulse has passed, and that such waveguiding effect can be used for long-term guiding of another beam. We estimate the peak value of this positive index change to be $\sim 10^{-6}$, as this is the value required to form a single-mode waveguide where the diameters of the guided mode and the waveguide are $\sim 100 \mu\text{m}$.

The physical mechanism giving rise to the positive index change and to the waveguiding effect is still unknown. We mention here three options: (1) High density of air, (2) a temperature increase that excites the molecules into higher energy levels and therefore increase their polarizability, and (3) population of negative ions [25] with large polarizability. Option 1 (high density of air), may results from the following chain of events. The femtosecond pulse transfers heat to the air, increasing its temperature and leading to a central region with relative low pressure. Then, the air cools down and a wind blows towards the center in order to balance the pressures. Consequently, a spike of higher air density is formed in the center. This scenario is somewhat analogous to the formation of Worthington Jets [24].

Next, we move to presenting the formation and outgoing propagation of pulse radial sound-waves produced in the wake of the filaments. Notably, the formation of the acoustic waves from laser filaments has not been explored before. The acoustic wave is formed during the same time-window as the central spike with positive index change. The formation of the leading ring crest of the acoustic pulse is seen in Figs. 2(a-f) and

also in Fig. 4a which shows line cuts of Figs. 2(d,e,f). Figure 4b shows the calculated radius of the leading crest as a function of Δt . Interestingly, the leading crest is formed at 0.08 μsec , yet it starts to propagate at 0.3 μsec delay times. The second and third crest rings are formed at 0.78 μsec and 0.62 μsec delay times, respectively. Finally, Fig. 5 shows the outgoing propagation of the sound wave. Figures 5(a-e) show the intensity of the probe beam (for a plane-wave launch configuration similar to that of Fig. 2) at the output plane, for several delay times. These plots clearly show the three-cycle acoustic pulse. Figure 5f shows the radius of the leading crest versus delay time from which we calculated the wave velocity to be 333 ± 1 m/s. This value is comparable to the sound velocity in air, thereby showing that the wave is indeed an acoustic wave. After the radial acoustic wave is emitted, a negative index change is left behind at the center. This negative index change, which decays slowly and is still observed even after a millisecond, was explored in Ref. 23.

In conclusions, we discovered that a filament induces a transient positive index-change that lasts for approximately 1.5 microsecond and demonstrated waveguiding through it. We also explored the formation and generation of the sound wave that results from the filament.

References

1. A. Braun, G. Korn, X. Liu, D. Du, J. Squier, and G. Mourou, *Opt. Lett.* 20, 73 (1995).
2. L. Berge, S. Skupin, R. Nuter, J. Kasparian and J-P. Wolf, *Rep. Prog. Phys.* 70 1633 (2007).
3. A. Couairon and A. Mysyrowicz, *Physics Reports* 441, 47 (2007).
4. M. Rodriguez, R. Bourayou, G. Méjean, J. Kasparian, J. Yu, E. Salmon, A. Scholz, B. Stecklum, J. Eislöffel, U. Laux, A. P. Hatzes, R. Sauerbrey, L. Wöste, and J.-P. Wolf, *Phys. Rev. E* 69, 036607 (2004).
5. J. Kasparian, M. Rodriguez, G. Méjean, J. Yu, E. Salmon, H. Wille, R. Bourayou, S. Frey, Y.-B. André, A. Mysyrowicz, R. Sauerbrey, J.-P. Wolf and L. Wöste, *Science*, 301, 61 (2003).
6. G. Méchain, A. Couairon, Y.-B. André, C. D'amico, M. Franco, B. Prade, S. Tzortzakis, A. Mysyrowicz, and R. Sauerbrey, *Appl. Phys. B: Lasers Opt.* B79, 379 (2004).
7. M. S. Mills, M. Kolesik, and D. N. Christodoulides, *Opt. Lett.*, 38, 25 (2013).
- Chin, S. L. et al. Filamentation of femtosecond laser pulses in turbulent air. *Appl. Phys. B* 74, 67–76 (2002).
8. R. Salame, N. Lascoux, E. Salmon, J. Kasparian and J.-P. Wolf, Propagation of laser filaments through an extended turbulent region. *Appl. Phys. Lett.* 91, 171106 (2007).
9. S.L. Chin et al., Filamentation of femtosecond laser pulses in turbulent air. *Appl. Phys. B* 74, 67 (2002).

10. Q. Luo et al., Appl. Phys. B82, 105 (2006).
11. P. Rohwetter et al., Nature Photonics 4, 451 (2010)
12. C. G. Durfee and H. M. Milchberg, Phys. Rev. Lett. 71, 2409 (1993).
13. C. G. Durfee, J. Lynch and H. M. Milchberg Phys. Rev. E 51, 2368 (1995).
14. S. Tzortzakis, B. Prade, M. Franco and A. Mysyrowicz, Opt. Commun. 181, 123 (2000).
15. P. K. Pandey, S. L. Gupta, V. Narayanan, and R.K. Thareja, Physics Of Plasmas 19, 023502 (2012).
16. M. Châteauneuf, S. Payeur, J. Dubois, and J.-C. Kieffer, Appl. Phys. Lett. 92, 091104 (2008).
17. C. D'Amico, A. Houard, M. Franco, B. Prade, A. Mysyrowicz, A. Couairon, and V. T. Tikhonchuk, Phys. Rev. Lett. 98, 235002 (2007).
18. B. Zhou et al., Optics Express 17, 11450 (2009).
19. H. Stapelfeldt and T. Seideman, Rev. Mod. Phys. 75, 543 (2003).
20. R. A. Bartels, T. C. Weinacht, N. Wagner, M. Baertschy, C. H. Greene, M. M. Murnane, and H. C. Kapteyn, Phys. Rev. Lett. 88, 013903 (2001).
21. S. Varma, Y. -H. Chen, and H. M. Milchberg, Phys. Rev. Lett. 101, 205001 (2008).
22. F. Calegari, C. Vozzi, and S. Stagira, Phys. Rev. A 79, 023827 (2009).
23. Y. -H. Cheng, J. K. Wahlstrand, N. Jhajj, and H. M. Milchberg, Optics Express, 21 4740 (2013).
24. A.L. Yarin, Annu. Rev. Fluid Mech. 38, 159 (2006).
25. B. Zhou et al., Optics Express 17, 11450 (2009).

Figures

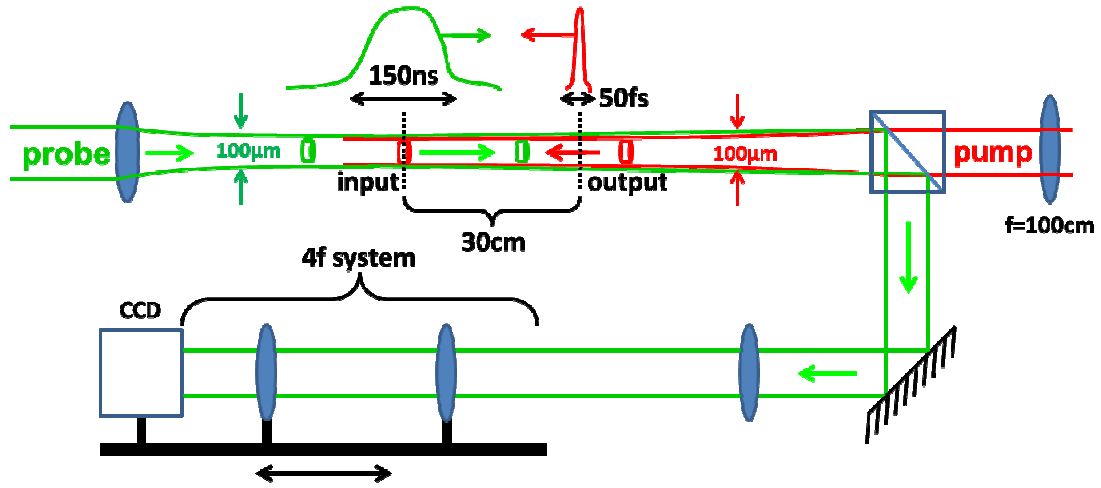


Figure 1: Scheme of the experimental setup. A Ti:Sapphire pulsed laser 1 cm wide beam with 50 fs time duration, 1 mJ energy/pulse at 1KHz repetition rate, is focused into a diameter of $\sim 100\ \mu\text{m}$, creating a filament of $\sim 30\ \text{cm}$ in the free air. The probe beam is a weak 527 nm pulse laser beam, with a duration time of 150 ns and repetition rate of 1KHz, triggered by the femtosecond laser. The delay between the pulses is controlled electronically and can span a range of one msec. In the filament region, the probe and pump beams propagate in opposite directions. The "input" and "output" planes correspond to the *probe* pulse entrance and exit planes of the filament channel, respectively. An imaging system images the probe pulse at the input and output planes. In the experiment presented in Fig. 3, we insert a lens that focuses the probe beam to a diameter of $\sim 100\ \mu\text{m}$ at the input plane. No focusing lens is used in the experiments presented in Figs. 2 and 4, hence the probe beam is approximately a plane wave.

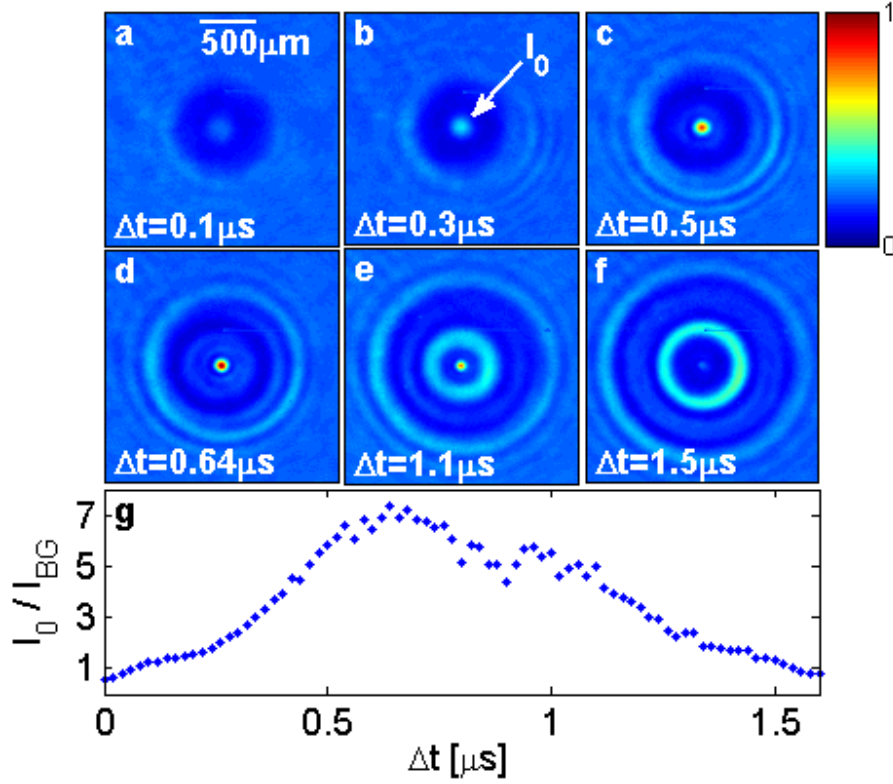


Figure 2: Long-lived positive index change in the filament wake. Shown are the intensity structures of the probe beam at the output plane, for delay times of $\Delta t = 0.1$ (a), $\Delta t = 0.3$ (b), $\Delta t = 0.5$ (c), $\Delta t = 0.64$ (d), $\Delta t = 1.1$ (e) and $\Delta t = 1.5$ (f) microseconds - after the filamenting pulse. (g) Ratio between the peak intensity at the center (I_0 which is pointed by an arrow in Fig. 2b) and the background intensity versus the delay time between the probe and pump pulses (here, $\Delta t = 0$ corresponds to time delay for which the probe and pump pulses collide within the filament channel). The outer ring that forms in (a) and subsequently expands and becomes stronger (b-f) reflects an acoustic density wave discussed in Figs. 4 and 5.

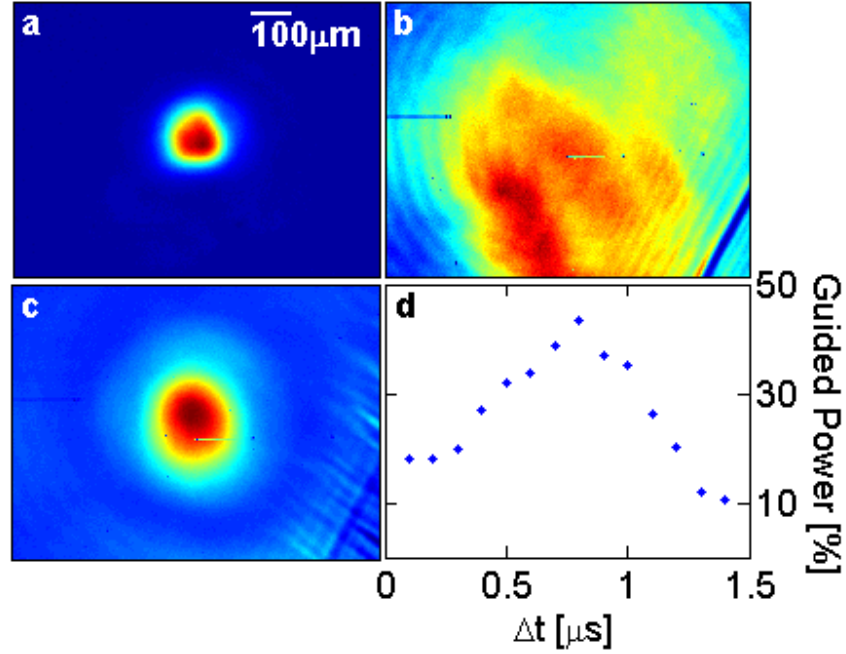


Figure 3: Long-lived filament-induced waveguide. (a) Intensity structure of the focused probe beam at the input plane. (b) Intensity structure of the probe beam at the output plane when the pump beam is blocked, i.e. no filament is formed. In the absence of the filament, the probe beam exhibits considerable diffraction broadening. (c) Intensity structure of the guided probe beam at the output plane for delay time of 800 ns with respect to the filamenting pulse. (d) The fraction of power localized within the guiding region (a circle with 300 μm diameter). In Figs 3(a-c), each plot is normalized separately. The line in the lower right corners of Figs 3(b,c) corresponds to a wire that we used for spotting the output plan.

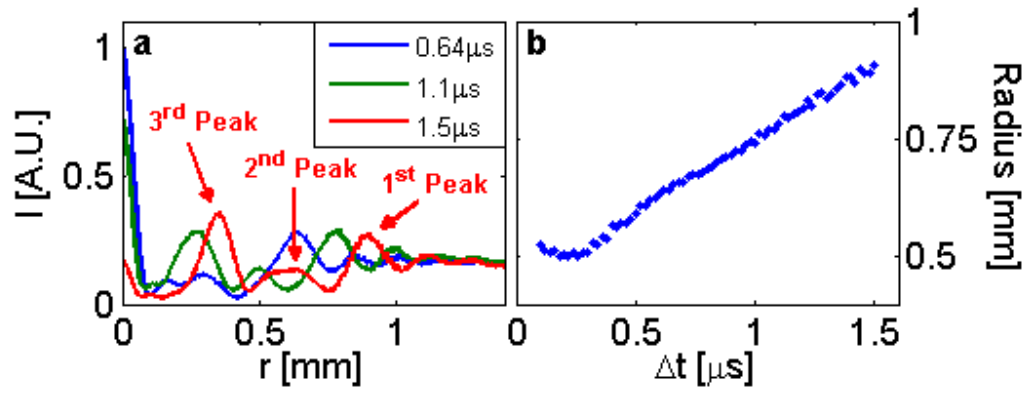


Figure 4: Formation of the acoustic pulse. (a) 1D Intensity profiles of the probe beam at the output plane at 0.64, 1.1 and 1.5 microseconds delay times. (b) Radius of the first ring crest as a function of time delay.

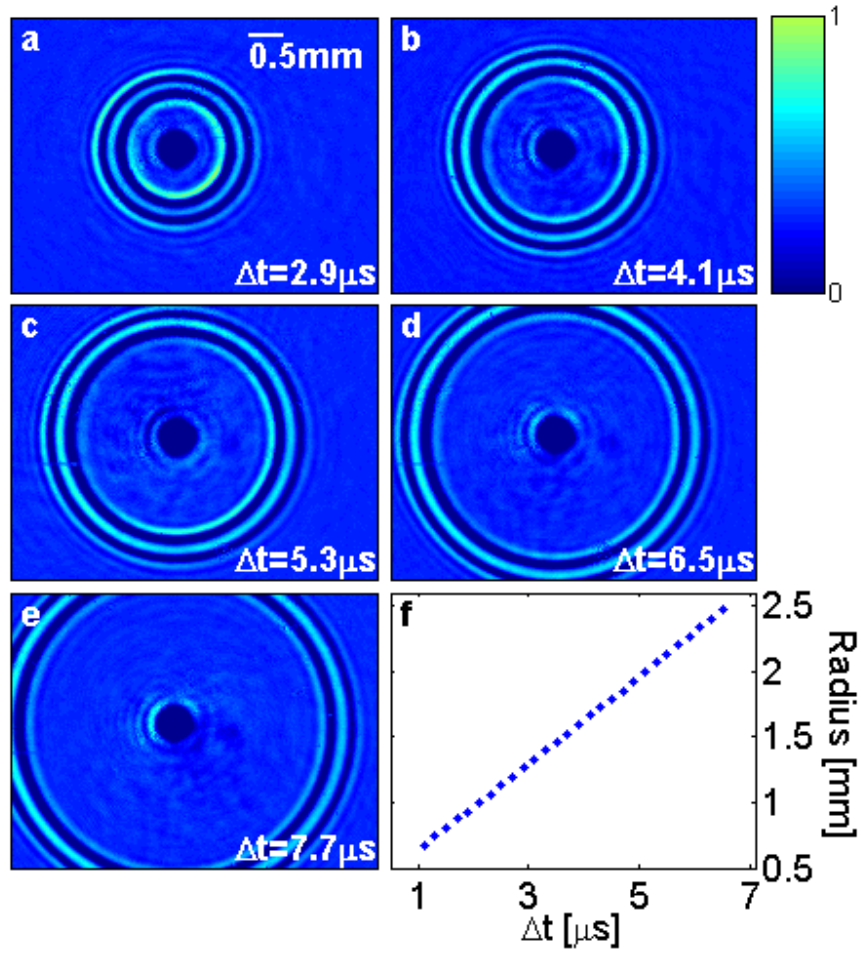


Figure 5: Outward propagation of the acoustic pulse. Shown are the intensity structures of the probe beam (plane wave) at the output plane for delay times of $\Delta t=2.9$ (a), $\Delta t=4.1$ (b), $\Delta t=5.3$ (c) $\Delta t=6.5$ (d) and $\Delta t=7.7$ (e) microseconds after the filamenting pulse. (f) Radius of the leading crest versus delay time. The calculated angle of the line corresponds to a velocity of 333 ± 1 m/s.